Supplementary Information to

‘Effect of the synthetic route on the structural, textural, morphological and catalytic properties of Iron(III) oxides and oxyhydroxides’

Paula Oulego[a], María A. Villa-García[b], Adriana Laca [a]and Mario Diaz[a]*

[a]Department of Chemical and Environmental Engineering, University of Oviedo.

[b]Department of Organic and Inorganic Chemistry, University of Oviedo.

c/Julián Clavería, s/n, 33071, Oviedo, Spain

(29 Pages, 5 Tables, 2 Figures)

Table of contents

1. **Instrumental parameters for the determination of the iron content by ICP-MS (Table S1).**
2. **Determination of bacterial toxicity of the landfill leachate treated by catalytic wet oxidation.**
3. **Determination of the color number (CN) of the landfill leachate treated by catalytic wet oxidation.**
4. **Selected electron diffraction pattern (SAED) of hematite H1 (Figure S1).**
5. **EDX analysis of the iron(III) oxides and oxyhydroxides (Figure S2).**
6. **Comparison of the data of this study with those found in the literature (Table S2 to S5).**
7. **References**

*Corresponding author’s e-mail: mavg@uniovi.es (M.A. Villa-García)
Phone: +34 985 10 29 76; Fax: +34 985 10 34 46

1. Instrumental parameters for the determination of the iron content by ICP-MS (Table S1).

Table S1. Instrumental parameters for ICP-MS.

Inductively Coupled Plasma		Mass Spectrometer	
RF power (W)	1500	Sampling cone	Nickel
Carrier gas (L/min)	1.12	Skimmer cone	Nickel
Plasma gas (L/min)	15	Data acquisition	3 points per mass
Auxiliary gas (L/min)	1.0	Integration time	0.1 s per point
Sample depth (mm)	8	Acquisitions	5
Solution uptake rate (mL/min)	0.4	Analytical masses	^{57}Fe and ^{103}Rh
Nebulizer	Babington type		

2. Determination of bacterial toxicity of the landfill leachate treated by catalytic wet oxidation

The assessment of bacterial toxicity was carried out with *Vibrio fischeri*. The commercial assay Biofix®Lumi-10 (Macherey-Nagel, Germany) was employed using a freeze-dried specially selected strain of the marine bacterium (NRRL number B-11177). Toxicity was evaluated in samples diluted 1:5 and results were given as inhibition percentage (LI) according to ISO 11348-3. The drop in light emission of the bacteria after a contact period of 15 min was measured and compared with a sample of control free of toxicants (2% NaCl solution). Temperature was kept at 15 ºC by a thermo block and sample salinity was adjusted to 2% after adjusting the sample pH between 6.5 and 7.5.

3. Determination of the color number (CN) of the landfill leachate treated by catalytic wet oxidation

As it was previously commented in the manuscript, the color number (CN), was employed to monitor changes in the color of the leachate during its oxidation, its value was calculated using equation S1. Spectral absorbance coefficients (SAC) are defined as the ratio of the values of the respective absorbance (Abs) over the cell thickness (x) (see equation S2). This parameter was measured at 436, 525 and 620 nm using a UV/Vis spectrophotometer (Thermo Scientific, Heλios γ).

$$CN = \frac{SAC_{436}^2 + SAC_{525}^2 + SAC_{620}^2}{SAC_{436} + SAC_{525} + SAC_{620}} \quad \text{(S1)}$$

$$SAC_i = \frac{Abs_i}{x} \quad \text{(S2)}$$

4. Selected electron diffraction pattern (SAED) of hematite H1 (Figure S1).

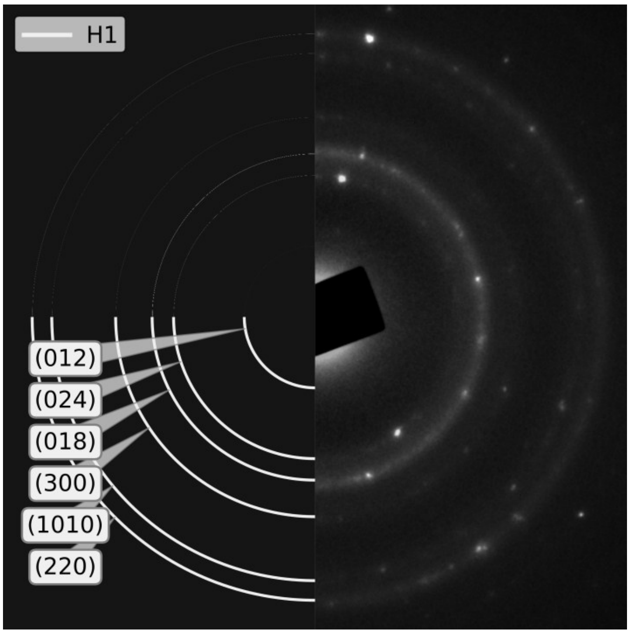

Figure S1. Electron diffraction pattern of hematite H1 (right) and simulated electron diffraction pattern of the rhomboedral hematite JCPDS no. 33-0664 (left).

5. EDX analysis of the iron(III) oxides and oxyhydroxides (Figure S2).

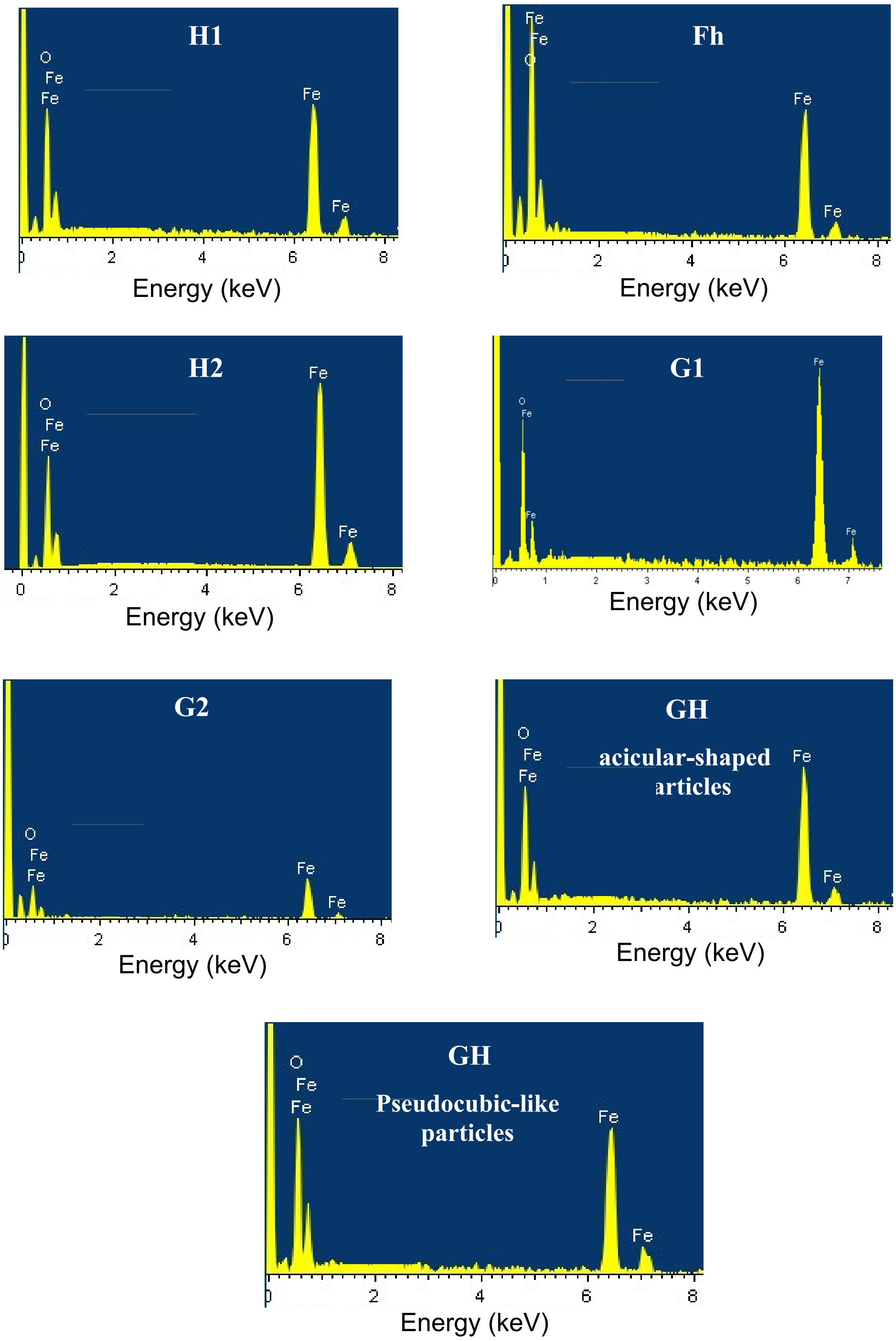

Figure S2. EDX analysis of the iron(III) oxides and oxyhydroxides.

6. Comparison of the data of this study with those found in the literature (Table S2 to S5).

Table S2. Comparison of X-ray diffraction data obtained in this study with those found in the literature.

	Results of this study				*Data found in the literature*			
Sample	***XRD peaks of the solids***	***Miller indices (hkl)***	***Iron-bearing phase***	***Crystallinity of the solids of this study***	***Miller indices (hkl)***	***Iron-bearing phase***	***Crystallinity of the solids of this study***	***Reference***
Hematite	Solid H1: 24.1º, 35.7º, 49.5º, 57.8º, 62.6º, 72.1º and 75.4º	Solid H1: (012), (110), (024), (018), (300), (1010), (220)	Rhombohedral hematite: JCPDS no. 33-0664.	Very poorly ordered material.	• Hematite nanospheres[1]: (012), (104), (110), (113), (024), (116), (018), (214), (300) • Hematite nanocubes[2] and thin film[3]: (012), (104), (110), (113), (024), (116), (018), (214), (300), (1010) • Hematite nanocubes[4]:	Rhombohedral hematite: JCPDS no. 33-0664.	• Hematite nanospheres[1]: crystalline. • Hematite nanocubes[2,4]: highly crystalline. • Hematite thin film[3]: crystalline.	[1]Tadic et al., 2012; [2]Qin et al., 2011; [3]Hamd et al., 2012; [4]Chernyshova et al., 2010.

					(012), (104), (110), (006), (113), (200), (024), (116), (018), (214), (300), (208)			

Table S2. Comparison of X-ray diffraction data obtained in this study with those found in the literature (continuation).

	Results of this study				***Data found in the literature***			
Sample	***XRD peaks of the solids***	***Miller indices (hkl)***	***Iron-bearing phase***	***Crystallinity of the solids of this study***	***Miller indices (hkl)***	***Iron-bearing phase***	***Crystallinity of the solids of this study***	***Reference***
Hematite	Solid H2: 24.1º, 33.4º, 35.7º, 41.1º, 49.5º, 54.2º, 62.6º, 64.1º, 72.1º and 75.4º	Solid H2: (012), (104), (110), (113), (024), (116), (214), (300), (1010), (220)	Rhombohedral hematite: JCPDS no. 33-0664.	Poorly ordered material and/or presence of very fine hematite	• Hematite nanospheres[1]: (012), (104), (110), (113), (024), (116), (018), (214), (300) • Hematite nanocubes[2] and thin film[3]:	Rhombohedral hematite: JCPDS no. 33-0664.	• Hematite nanospheres[1]: crystalline. • Hematite nanocubes[2,4]: highly. crystalline	[1]Tadic et al., 2012; [2]Qin et al., 2011; [3]Hamd et al., 2012; [4]Chernyshova et al.,

				particles	(012), (104), (110), (113), (024), (116), (018), (214), (300), (1010) • Hematite nanocubes[4]: (012), (104), (110), (006), (113), (200), (024), (116), (018), (214), (300), (208)		• Hematite thin film[3]: crystalline.	2010.

Table S2. Comparison of X-ray diffraction data obtained in this study with those found in the literature (continuation).

	Results of this study				***Data found in the literature***			
Sample	***XRD peaks of the solids***	***Miller indices (hkl)***	***Iron-bearing phase***	***Crystallinity of the solids of this study***	***Miller indices (hkl)***	***Iron-bearing phase***	***Crystallinity of the solids of this study***	***Reference***

Ferrihy-drite	Solid Fh:35.7º and 63.5º	Solid Fh: (110), (300)	No single formula is widely accepted. $Fe_{10.4}O_{14.2}(OH)_2$	Poorly ordered material.	• 2-line ferrihydrite[5,6]: (110), (300)	$Fe_{10}O_{14}(OH)_2$[5] $Fe_5HO_8\cdot 4H_2O$[6] ; $5Fe_2O_3\cdot 9H_2O$[6,7];	Poorly crystalline.[5-7]	[5]Michel et al., 2007; [6]Tüysüz et al., 2011; [7]Fleischer et al., 1975.

Table S2. Comparison of X-ray diffraction data obtained in this study with those found in the literature (continuation).

	Results of this study				***Data found in the literature***			
Sample	***XRD peaks of the solids***	***Miller indices (hkl)***	***Iron-bearing phase***	***Crystallinity of the solids of this study***	***Miller indices (hkl)***	***Iron-bearing phase***	***Crystallinity of the solids of this study***	***Reference***

Goethite	Solid G1: 17.9º, 21.2º, 26.1º,33.2º, 33.5º, 36.7º, 40.3º, 41.4º, 45.5º, 47.6º, 50.9, 53.1º, 57.6º, 59.1º, 61.5º, 64.7º, 69.3º, 71.7º and 75.4º	Solid G1: (020), (110), (120), (130), (021), (111), (121), (140), (131), (041), (211), (221), (231), (151), (002), (061), (112), (170), (132)	Orthorhombic phase of goethite: JCPDS no. 29-0713.	Highly crystalline.	• Goethite rods[8,9]: (020), (110), (120), (130), (021), (040), (111), (200), (121), (140), (211), (221), (240), (231), (151), (160), (020), (161) • Acicular goethite[10]: (020), (110), (120), (130), (021), (040), (111), (200), (121), (140), (211), (221)	Orthorhombic phase of goethite: JCPDS no. 29-0713.	Goethite rods: highly crystalline.[8,9] Acicular goethite: highly crystalline.[10]	[8]Ristić et al., 2015; [9]Wei et al., 2012; [10]Montes-Hernandez et al., 2011.

Table S2. Comparison of X-ray diffraction data obtained in this study with those found in the literature (continuation).

	Results of this study				***Data found in the literature***			
Sample	***XRD peaks***	***Miller indices (hkl)***	***Iron-bearing***	***Crystallinity***	***Miller indices (hkl)***	***Iron-bearing***	***Crystallinity***	***Reference***

	of the solids		***phase***	***of the solids of this study***		***phase***	***of the solids of this study***	
Goethite	Solid G2: 17.9º, 21.2º, 26.1º,33.2º, 33.5º, 36.7º, 40.3º, 41.4º, 47.6º, 50.9, 53.1º, 57.6º, 59.1º, 61.5º, 64.7º, 69.3º, 71.7º and 75.4º	Solid G2: (020), (110), (120), (130), (021), (111), (121), (140), (041), (211), (221), (231), (151), (002), (061), (112), (170), (132)	Orthorhombic phase of goethite: JCPDS no. 29-0713.	Highly crystalline	• Goethite rods[8,9]: (020), (110), (120), (130), (021), (040), (111), (200), (121), (140), (211), (221), (240), (231), (151), (160), (020), (161) • Acicular goethite[10]: (020), (110), (120), (130), (021), (040), (111), (200), (121), (140), (211), (221)	Orthorhombic phase of goethite: JCPDS no. 29-0713.	Goethite rods: highly crystalline.[8,9] Acicular goethite: highly crystalline.[10]	[8]Ristić et al., 2015; [9]Wei et al., 2012; [10]Montes-Hernandez et al., 2011.

Table S2. Comparison of X-ray diffraction data obtained in this study with those found in the literature (continuation).

	Results of this study	***Data found in the literature***

Sample	***XRD peaks of the solids***	***Miller indices (hkl)***	***Iron-bearing phase***	***Crystallinity of the solids of this study***	***Miller indices (hkl)***	***Iron-bearing phase***	***Crystallinity of the solids of this study***	***Reference***
Mixture of hematite and goethite	Solid GH: • Hematite: 24.1°, 33.4°, 35.7°, 41.1°, 49.5°, 54.2°, 62.6°, 64.1°, 72.1° and 75.4° • Goethite: 36.7°, 53.3°, 57.6° and 59.2°	Solid GH: • Hematite: (012), (104), (110), (113), (024), (116), (214), (300), (1010), (220) • Goethite: (111), (221), (231), (151)	• Rhombohedral hematite: JCPDS no. 33-0664. • Orthorhombic phase of goethite: JCPDS no. 29-0713.	Both phases highly crystalline	• Hematite nanocubes[4] (012), (104), (110), (113), (024), (116), (018), (214), (300), (1010) • Goethite rods[8,9] (020), (110), (120), (130), (021), (040), (111), (200), (121), (140), (211), (221), (240), (231), (151), (160), (020), (161)	• Rhombohedral hematite: JCPDS no. 33-0664. • Orthorhombic phase of goethite: JCPDS no. 29-0713.	• Hematite nanocubes[4]: highly crystalline. • Goethite rods: highly crystalline.[8,9]	[4]Chernyshova et al., 2010. [8]Ristić et al., 2015; [9]Wei et al., 2012.

Table S3. Comparison of Mössbauer data obtained in this study with those found in the literature.

	Results of this study			**Data found in the literature**			
Sample	***Doublet***	***Isomer shift*** (δ) $mm \cdot s^{-1}$	***Quadrupole splitting*** (ΔE_Q)	***Doublet***	***Isomer shift*** (δ) $mm \cdot s^{-1}$	***Quadrupole splitting*** (ΔE_Q)	***Reference***
Ferrihydrite (Fh)	Single Paramagnetic	0.35	0.62	Paramagnetic	0.33[11] 0.35[12]	0.62[11] 0.63[12]	[11]Ristić et al., 2007; [12]Murad, 1996.
Hematite (H1)	Paramagnetic	0.35	0.72	Paramagnetic	0.35[13] 0.33[14] 0.33-0.35[15]	0.68[13] 0.75[14] 0.80[15]	[13]Pariona et al., 2016; [14]Mashlan et al., 2004; [15]Zboril et al., 2002.

Table S4. Comparison of FT-IR data obtained in this study with those found in the literature.

	Results of this study					***Data found in the literature***					
Sample	***OH stretching vibrations (cm^{-1})***	***OH bending vibrations (cm^{-1})***	***Lattice vibrations (cm^{-1})***	***Carbonate species stretching vibrations (cm^{-1})***	***Characteristic vibrations (cm^{-1})***	***OH stretching vibrations (cm^{-1})***	***OH bending vibrations (cm^{-1})***	***Lattice vibrations (cm^{-1})***	***Carbonate species stretching vibrations (cm^{-1})***	***Characte-ristic vibrations (cm^{-1})***	***Reference***
Ferrihy-drite (Fh)	3400	1636	668	1384, 1108	580, 452	3420-3357[11]	1623-1620[11]	660[11] <700[16]	1352[11] 1360[17], 1070[17]	580, 441[11]	[11]Ristić et al., 2007; [16]Krehula and Musić, 2008; [17]Su and Suarez,1997
Hematite (H1 and H2)	3434	1636	668	1540 1384	532, 445	3420-3357[11]	1623-1620[11]	660[11]	1490[17], 1360[17]	526,440[18]	[11]Ristić et al., 2007; [16]Krehula and Musić, 2008 [17]Su and Suarez, 1997;

											[18]Jubb et al., 2010

Table S4. Comparison of FT-IR data obtained in this study with those found in the literature (continuation).

	Results of this study					***Data found in the literature***					
Sample	***OH stretching vibrations (cm^{-1})***	***OH bending vibrations (cm^{-1})***	***Lattice vibrations (cm^{-1})***	***Carbonate species stretching vibrations (cm^{-1})***	***Characteristic vibrations (cm^{-1})***	***OH stretching vibrations (cm^{-1})***	***OH bending vibrations (cm^{-1})***	***Lattice vibrations (cm^{-1})***	***Carbonate species stretching vibrations (cm^{-1})***	***Characte-ristic vibrations (cm^{-1})***	***Reference***
Goethite (G1 and G2)	3434[a], 3136[b]	1636	668	1384, 1111	894[c], 796[d], 636[e], 457[f]	3420-3357[a,11] 3144[b,18]	1620-1623[11]	660[11] <700[16]	1352[11] 1360[17], 1070[17]	895-884[c,19,20], 800-798[d,19,20] 622-617[e,20] 461-454[f,20]	[11]Ristić et al., 2007; [16]Krehula and Musić, 2008; [17]Su and Suarez,1997; [18]Jubb et al., 2010; [19]Gotić and Musić, 2007;

											[20]Ruan et al., 2001.

[a]Physically adsorbed water molecules; [b]in the goethite structure; [c]Fe-O-H vibration in-plane; [d]Fe-O-H vibration out-of-plane; [e]FeO_6 vibration in the a-plane; [f]FeO_6 vibration in the b-c-plane.

Table S4. Comparison of FT-IR data obtained in this study with those found in the literature (continuation).

	Results of this study					**Data found in the literature**					
Sample	***OH stretching vibrations (cm^{-1})***	***OH bending vibrations (cm^{-1})***	***Lattice vibrations (cm^{-1})***	***Carbonate species stretching vibrations (cm^{-1})***	***Characteristic vibrations (cm^{-1})***	***OH stretching vibrations (cm^{-1})***	***OH bending vibrations (cm^{-1})***	***Lattice vibrations (cm^{-1})***	***Carbonate species stretching vibrations (cm^{-1})***	***Characte-ristic vibrations (cm^{-1})***	***Reference***
Mixture of hematite and goethite (GH)	3447	1636	668	1384, 1112	894[a], 796[b], 560[c], 480[c]	3420-3357[11]	1620-1623[11]	660[11] <700[16]	1352[11] 1360[17], 1070[17]	895-884[a,19,20], 800-798[b,19,20], 580[c,11], 441[c,11]	[11]Ristić et al., 2007; [16]Krehula and Musić, 2008; [17]Su and Suarez,1997; [19]Gotić and Musić, 2007; [20]Ruan et al., 2001.

[a]Fe-O-H vibration in-plane; [b]Fe-O-H vibration out-of-plane; [c]Bands which are the fingerprint of hematite (morphological effects can vary the positions of these bands).

Table S5. Comparison of textural characterization and microstructure of the solids obtained in this study with those found in the literature.

	Synthetic route[a]					***Data found in the literature***					
Sample	***Iron source***[b]***; Additive***[c]	***Method***[d]	***pH***	***T of ageing (ºC)***	***Time (h)***	***BET surface area (m²/g)***	***Average pore size (nm)***	***Pore Volume (cm³/g)***	***Particle Size: TEM(nm)***	***Morphology***	***Reference***
Hematite	Fe(III) salt; No additive	Precipitation	n.a.	20	4	n.a.	n.a.	n.a.	Average: 50-100	Irregular	[21]Paul et al., 2015
Hematite	Fe(III) salt; With additives	Precipitation	n.a.	20	4	244.8 - 276.2	8.83-9.74	0.596 - 0.609	Average:2-50	Quasi spherical	[21]Paul et al., 2015

[a]Implying batch system. [b]Fe(III) salt: $Fe(NO_3)_3 \cdot 9H_2O$. [c]Additives: *PEG 400 or PEG 4000*. [d]Precipitating agent: $(CH_2)_6N_4$
n.a.: Not reported.

Table S5. Comparison of textural characterization and microstructure of the solids obtained in this study with those found in the literature (continuation).

	Synthetic route[a]					***Data found in the literature***					
Sample	***Iron source***[b]***; Additive***	***Method***[c]	***pH***	***T of ageing (°C)***	***Time (h)***	***BET surface area (m²/g)***	***Average pore size (nm)***	***Pore Volume (cm³/g)***	***Particle Size: TEM***[d] ***or Scherrer***[e] ***(nm)***	***Morphology***	***Reference***
Hematite	Fe(III) salt; No additive	Precipitation	n.a.	20	4	n.a.	n.a.	n.a.	Average [e]: 31	Spheroidal	[22]Sivakumar et al., 2014
Hematite	Fe(III) salt; No additive	Precipitation (under pure N_2 gas)	7	>100	1	18.5-55.4	n.a.	n.a.	Average [d]: 50-150	Spherical, cubic and ellipsoidal	[23]Supatta-rasakda et al., 2013

[a]Implying batch system. [b]Fe(III) salt: $FeCl_3 \cdot 6H_2O$. [c]Precipitating agent: NaOH
n.a.: Not reported.

Table S5. Comparison of textural characterization and microstructure of the solids obtained in this study with those found in the literature (continuation).

	Synthetic route[a]					***Data found in the literature***					
Sample	***Iron source***[b]***; Additive***	***Method***[c]	***pH***	***T of ageing (°C)***	***Time (h)***	***BET surface area (m²/g)***	***Average pore size (nm)***	***Pore Volume (cm³/g)***	***Particle Size: TEM (nm)***	***Morphology***	***Reference***
Hematite	Fe(III) salt; No additive	Precipitation	7	>100	n.a.	17.18-31.83	n.a.	n.a.	Average: 60-80	Quasi-spherical	[24]Liu et al., 2007
Hematite	Fe(III) salt; No additive	Precipitation	H1: 9	H1: 20	H1:3	H1: 291.4	H1: 3.32-3.97	H1:0.328	H1(average): 4	H1: Spheroidal	This study
			H2: 12	H2: 20	H2:3	H2: 118.3	H2: 5.77-6.20	H2:0.188	H2: widely variable	H2: amorphous	

[a]Implying batch system. [b]Fe(III) salt: $FeCl_3 \cdot 6H_2O$ or $Fe(NO_3)_3 \cdot 9H_2O$. [c]Precipitating agent: NaOH or NH_4OH
n.a.: Not reported.

Table S5. Comparison of textural characterization and microstructure of the solids obtained in this study with those found in the literature (continuation).

	Synthetic route[a]					***Data found in the literature***					
Sample	***Iron source***[b]***; Additive***	***Method***	***pH***	***T of ageing (ºC)***	***Time (h)***	***BET surface area (m^2/g)***	***Average pore size (nm)***	***Pore Volume (cm^3/g)***	***Particle Size: TEM (nm)***	***Morphology***	***Reference***
Ferrihy-drite	Fe(III) salt; cyclohexane, polyethylene-glycol, ammonia solution and isopropanol	Micro-emulsion	n.a.	50	3	390	5.6	0.54	n.a.	n.a.	[25]Xu et al., 2013
Ferrihy-drite	Fe(III) salt; cyclohexane, polyethylene-glycol, ammonia solution and isopropanol	Micro-emulsion	n.a.	50	3	97	9.3	0.25	Average : 10	spherical	[26]Yan et al., 2015

[a]Implying batch system. [b]Fe(III) salt: $FeCl_3$.
n.a.: Not reported.

Table S5. Comparison of textural characterization and microstructure of the solids obtained in this study with those found in the literature (continuation).

	Synthetic route[a]					***Data found in the literature***					
Sample	***Iron source***[b]***; Additive***	***Method***	***pH***	***T of ageing (^{o}C)***	***Time (h)***	***BET surface area (m^2/g)***	***Average pore size (nm)***	***Pore Volume (cm^3/g)***	***Particle Size: TEM (nm)***	***Morphology***	***Reference***
Ferrihy-drite	Fe(III) salt; brij 58, isopropyl alcohol and ammonia solution	Micro-emulsion	8	55	72	192.3	5.00-5.54	0.341	Average: 7	Spheroidal	This study (solid Fh)

[a]Implying batch system. [b]Fe(III) salt: $Fe(NO_3)_3 \cdot 9H_2O$.

Table S5. Comparison of textural characterization and microstructure of the solids obtained in this study with those found in the literature (continuation).

	Synthetic route[a]					***Data found in the literature***					
Sample	***Iron source***[b]***; Additive***[c]	***Method***[d]	***pH***	***T of ageing (°C)***	***Time (h)***	***BET surface area (m^2/g)***	***Average pore size (nm)***	***Pore Volume (cm^3/g)***	***Particle Size: FESEM***[e] ***or TEM***[f] ***(nm)***	***Morphology***	***Reference***
Goethite	Fe(III) salt; No additive	Sol-gel	2.5-13.5	30	24	133.80	n.a.	n.a.	Length[e]: 250±35 Width[e]: 65±20	low acicular	[10]Montes-Hernández et al., 2011
Goethite	Fe(III) salt; With additive	Sol-gel	3.0	90	1	n.a.	n.a.	n.a.	Largest dimension [f]: 1-10	Irregular	[27]Mohapatra et al., 2009

[a]Implying batch system. [b]Fe(III) salt: $Fe(NO_3)_3 \cdot 9H_2O$ or $FeCl_3 \cdot 6H_2O$ [c]Additive: hydrazine sulphate. [d]Alkaline source: NaOH or $Ca(OH)_2$.

n.a.: Not reported.

Table S5. Comparison of textural characterization and microstructure of the solids obtained in this study with those found in the literature (continuation).

	Synthetic route[a]					***Data found in the literature***					
Sample	***Iron source***[b]***; Additive***[c]	***Method***	***pH***	***T of ageing (ºC)***	***Time (h)***	***BET surface area (m^2/g)***	***Average pore size (nm)***	***Pore Volume (cm^3/g)***	***Particle Size: TEM (nm)***	***Morphology***	***Reference***
Goethite	Fe(III) salt; No additive	Sol-gel[d]	11-12	25-120	48-288	n.a.	n.a.	n.a.	Length: 202 to 282; Width: 16 to 86	Rod or Lath-like particles	[28]Thies-Weesie et al., 2007

Goethite	Fe(III) salt; With additives	Micro-emulsion and precipitation[e]	n.a.	90	2-6	n.a.	n.a.	n.a.	Length: 60 to 150; Width: 7	Nanotubes	[29]Yu et al., 2007

[a]Implying batch system. [b]Fe(III) salt: $Fe(NO_3)_3 \cdot 9H_2O$ or $FeCl_3$ [c]Additives: hydrazine sulphate, oleic acid, and xylene. [d]Alkaline source: NaOH or NH_4OH [e]Precipitating agent: CH_3CH_2OH.
n.a.: Not reported.

Table S5. Comparison of textural characterization and microstructure of the solids obtained in this study with those found in the literature (continuation).

	Synthetic route[a]					***Data found in the literature***					
Sample	***Iron source***[b]***; Additive***[c]	***Method***	***pH***	***T of ageing (°C)***	***Time (h)***	***BET surface area (m^2/g)***	***Average pore size (nm)***	***Pore Volume (cm^3/g)***	***Particle Size: TEM (nm)***	***Morphology***	***Reference***
Goethite	Fe(III) salt; With additive	Sol-gel[d]	12	90	72	n.a.	n.a.	n.a.	Length:90-152; Width:10-14	Nanorods	[30]Lee Penn et al., 2006

Goethite	Fe(III) salt; No additive	Precipitation[e]	1.7-8	25	> 0.25	280-316	1.7-8.8	0.22-0.47	Largest dimension: 2-10	Spongy mass. Not well defined nanorods	[31]Bakoyannakis et al., 2003

[a]Dialysis (semicontinuous reactor). [b]Fe(III) salt: $Fe(NO_3)_3\cdot 9H_2O$, $FeCl_3\cdot 6H_2O$ or $Fe_2(SO_4)_3\cdot xH_2O$. [c]Additive: $NaHCO_3$. [d]Alkaline source (OH): NaOH. [e]Precipitating agent: $(NH_4)_2CO_3$ or $NH_2CO_2NH_4$.
n.a. Not reported.

Table S5. Comparison of textural characterization and microstructure of the solids obtained in this study with those found in the literature (continuation).

	Synthetic route[a]					***Data found in the literature***					
Sample	***Iron source[b]; Additive***	***Method[c]***	***pH***	***T of ageing (ºC)***	***Time (h)***	***BET surface area (m²/g)***	***Average pore size (nm)***	***Pore Volume (cm³/g)***	***Particle Size: TEM (nm)***	***Morphology***	***Reference***

Goethite	Fe(III) salt; No additive	Sol-gel	n.a.	80	48	40.20-47.05	n.a.	n.a.	n.a.	n.a.	[32]Kosmulski et al., 2003
Goethite	Fe(III) salt; No additive	Sol-gel	G1: 3-13	G1: 95	G1:168	G1: 51.3	G1: 28.36-32.20	G1:0.404	G1: Length: 400 ± 50; Width :15 ± 5	G1: Highly acicular	This study
			G2: 3-13	G2: 95	G2:168	G2: 53.6	G2: 22.07-23.95	G2:0.322	G2: Length: 950 ± 100; Width :140 ± 20	G2: Moderately acicular	

[a]Implying batch system. [b]Fe(III) salt: $Fe(NO_3)_3$ or $FeCl_3 \cdot 6H_2O$ [c]Precipitating agent: KOH or NaOH
n.a.: Not reported.

Table S5. Comparison of textural characterization and microstructure of the solids obtained in this study with those found in the literature (continuation).

	Synthetic route[a]					***Data found in the literature***					
Sample	***Iron source***[b]***; Additive***	***Method***[c]	***pH***	***T of ageing (ºC)***	***Time (h)***	***BET surface area (m^2/g)***	***Average pore size (nm)***	***Pore Volume (cm^3/g)***	***Particle Size: FESEM***[e]***or TEM***[f] ***(nm)***	***Morphology***	***Reference***
Mixture Goethite-Hematite	Fe(III) salt; No additive	Sol-gel	2.5-13.5	70	24	31.20	n.a.	n.a.	Length[e]: 750±100; Width[e]: 60±20	Highly acicular goethite; no data for hematite	[10]Montes-Hernández et al., 2011
Mixture Goethite-Hematite	Fe(III) salt; No additive	Sol-gel	3-13	95	168	13.2	27.74-31.56	0.102	Length[f]: 880±100; Width[f]: 145±50	Acicular (goethite); Pseudocubic (hematite)	This study (GH)

[a]Implying batch system. [b]Fe(III) salt: $Fe(NO_3)_3\cdot 9H_2O$ or $FeCl_3\cdot 6H_2O$. [c]Alkaline source: NaOH or $Ca(OH)_2$.
n.a.: Not reported.

7. References

1. M. Tadic, N. Citakovic, M. Panjan, B. Stanojevic, D. Markovic, Đ. Jovanovic and V. Spasojevic, *J. Alloy. Compd.*, 2012, **543**, 118-124.
2. W. Qin, C. Yang, R. Yi and G. Gao, *J. Nanomater.*, 2011, **2011**, 1-5.
3. W. Hamd, S. Cobo, J. Fize, G. Baldinozzi, W. Schwartz, M. Reymermier, A. Pereira, M. Fontecave, V. Artero, C. Laberty-Robert and C. Sanchez, *Phys. Chem. Chem. Phys.*, 2012, **14**, 13224-13232.
4. I. V. Chernyshova, S. Ponnurangam and P. Somasundaran, *Phys. Chem. Chem. Phys.*, 2010, **12**, 14045-14056.
5. F. M. Michel, L. Ehm, S. M. Antao, P. L. Lee, P. J. Chupas, G. Liu, D. R. Strongin, M. A. A. Schoonen, B. L. Phillips and J. B. Parise, *Science*, 2007, **316**, 1726-1729.
6. H. Tüysüz, E. L. Salabaş, C. Weidenthaler and F. Schüth, *J. Am. Chem. Soc.*, 2007, **130**, 280-287.
7. M. Fleischer, G. Y. Chao and A. Kato, *Am. Mineral.*, 1975, **60**, 485-489.
8. M. Ristić, I. Opačak, J. Štajdohar and S. Musić, *J. Mol. Struct.*, 2015, **1090**, 129-137.
9. C. Wei, P. Qiao, Z. Nan, *Mater. Sci. Eng*: C, 2012, **32**, 1524-1530.
10. G. Montes-Hernandez, P. Beck, F. Renard, E. Quirico, B. Lanson, R. Chiriac and N. Findling, *Cryst. Growth Des.,* 2011, **11**, 2264-2272.
11. M. Ristić, E. De Grave, S. Musić, S. Popović and Z. Orehovec, *J. Mol. Struct.*, 2007, **834–836**, 454-460.
12. E. Murad, *Phys. Chem. Miner.*, 1996, **23**, 248-262.
13. N. Pariona, K. I. Camacho-Aguilar, R. Ramos-González, A. I. Martinez, M. Herrera-Trejo and E. Baggio-Saitovitch, *J. Magn. Magn. Mater.*, 2016, **406**, 221-227.

14. M. Mashlan, R. Zboril, L. Machala, M. Vujtek, J. Walla and K. Nomura, *J. Metastab. Nanocryst.*, 2004, **20-21**, 641-647.
15. R. Zboril, M. Mashlan and D. Petridis, *Chem. Mater.,* 2002, **14**, 969-982.
16. S. Krehula and S. Musić, *J. Cryst. Growth*, 2008, **310**, 513-520.
17. C. Su and D. L. Suarez, *Clay. Clay. Miner.,* 1997, **45**, 814-825.
18. A. M. Jubb and H. C. Allen, *ACS Appl. Mater. Inter.*, 2010, **2**, 2804-2812.
19. M. Gotić and S. Musić, *J. Mol. Struct.*, 2007, **834–836**, 445-453.
20. H. D. Ruan, R. L. Frost and J. T. Kloprogge, *Spectrochim. Acta A*, 2001, **57**, 2575-2586.
21. B. Paul, B. Bhuyan, D. D. Purkayastha and S. S. Dhar, *Catal. Commun.*, 2015, **69**, 48-54.
22. S. Sivakumar, D. Anusuya, C. P. Khatiwada, J. Sivasubramanian, A. Venkatesan and P. Soundhirarajan, *Spectrochim. Acta Part A*, 2014, **128**, 69-75.
23. K. Supattarasakda, K. Petcharoen, T. Permpool, A. Sirivat and W. Lerdwijitjarud, *Powder Technol.*, 2013, **249**, 353-359.
24. H. Liu, Y. Wei, P. Li, Y. Zhang and Y. Sun, *Mater. Chem. Phys.*, 2007, **102**, 1-6.
25. Z. Xu, J. Yu and W. Xiao, *Chem – Eur. J.,* 2013, **19**, 9592-9598.
26. Z. Yan, Z. Xu, J. Yu and M. Jaroniec, *Environ. Sci. Technol.*, 2015, **49**, 6637-6644.
27. M. Mohapatra, K. Rout, S. K. Gupta, P. Singh, S. Anand and B. K. Mishra, *J. Nanopart. Res.*, 2009, **12**, 681-686.
28. D. M. E. Thies-Weesie, J. P. de Hoog, M. H. Hernandez Mendiola, A. V. Petukhov and G. J. Vroege, *Chem. Mater.*, 2007, **19**, 5538-5546.
29. T. Yu, J. Park, J. Moon, K. An, Y. Piao and T. Hyeon, *J. Am. Chem. Soc.*, 2007, **129**, 14558-14559.
30. R. Lee Penn, J. J. Erbs and D. M. Gulliver, *J. Cryst. Growth*, 2006, **293**, 1-4.

31. D. N. Bakoyannakis, E. A. Deliyanni, A. I. Zouboulis, K. A. Matis, L. Nalbandian and T. Kehagias, *Micropor. and Mesopor. Mat.*, 2003, **59**, 35-42.
32. M. Kosmulski, E. Maczka, E. Jartych and J. B. Rosenholm, *Adv. Colloid Interfac.*, 2003, **103**, 57-76.